ELSEVIER

Journal of Structural Geology 27 (2005) 495–502

JOURNAL OF STRUCTURAL GEOLOGY

www.elsevier.com/locate/jsg

Trishear modeling of fold bedding data along a topographic profile

Néstor Cardozo

Center for Integrated Petroleum Research, Allegaten 41, N-5007 Bergen, Norway

Received 16 December 2003; received in revised form 11 October 2004; accepted 11 October 2004
Available online 29 January 2005

Abstract

This paper describes an algorithm that extends the use of the trishear kinematic model to the commonly encountered case of a set of fold bedding observations along a profile. In a universe of trishear models that can possibly fit the structure, the algorithm searches for the model that minimizes the difference between observed and modeled beds (i.e. best fit model). The robustness and versatility of the algorithm are shown by applying it to a synthetic fold geometry, and to a transect of the Waterpocket monocline in southern Utah. In the first case, the best fit parameters are exactly those used in the synthetic model. In the second case, the best fit model reproduces fairly well the observable features of the monocline.

Keywords: Fault propagation folds; Trishear; Transect data

1. Introduction

Complete cross-sectional exposures or seismic images of fault propagation folds are rare. Commonly the data available for the folds are restricted to a narrow window close to the ground surface (a profile). In this window the data consist of a collection of bedding attitudes at different stratigraphic levels. One would like to reconstruct from these data locations the cross-sectional geometry of the fold and relate this geometry to the associated fault.

The flexural slip, kink dominated kinematic model (Suppe and Medwedeff, 1990) is ideal to perform this task: self-similarity (always the same fold shape and position relative to the propagating fault tip) and kink band migration provide a set of rules to graphically 'fill' the space below the profile.

Fault propagation folds, however, commonly depart from the self-similar, kink band picture. The folds usually display changes in stratigraphic thickness and dip on their forelimbs, footwall synclines, and both rounded and angular fold hinges. Fold geometries change with structural level and proximity to the fault tip.

The trishear kinematic model (Erslev, 1991) can better explain these features. In trishear, folding develops incrementally in a triangular zone of distributed shear that expands ahead of the propagating fault tip. Complex fold geometries and strain fields result from a combination of five model parameters: ramp angle, apical angle of the triangular zone of shear (trishear angle), fault slip, fault propagation to fault slip ratio (P/S), and location of the fault tip (Allmendinger, 1998). Trishear, however, presents a fundamental problem in the modeling of real structures. The model must be applied numerically rather than graphically. Knowledge of the current fold geometry relies on knowledge of the incremental evolution of the fold.

Allmendinger (1998) devised an ingenious solution to this problem. Taking advantage of the fact that trishear can be run backwards (inverse modeling), he implemented an algorithm that inverts for the combination of trishear parameters that best 'restore' one bed in the section to its original planar orientation. The success of his method depends on the geologist having good control of at least one bed across the entire fold. This condition, unfortunately, is rarely achieved.

This paper describes an algorithm that extends the capabilities of trishear modeling to the frequently encountered case of a set of beds outcropping along a topographic profile. The robustness of the algorithm is tested by applying it to a forward trishear model generated with precisely

E-mail address: nestor.cardozo@ngi.no.

0191-8141/$ - see front matter © 2005 Published by Elsevier Ltd.
doi:10.1016/j.jsg.2004.10.004

known trishear parameters. The versatility of the algorithm is then demonstrated by applying it to the Waterpocket monocline in southern Utah.

2. Method

The algorithm relies on a forward modeling approach. The basic question posed in this problem is: given bedding data from a series of observations along a profile, how can one choose from a universe of forward trishear models (i.e. universe of fold geometries), the model (i.e. set of folded beds) that is most consistent with the data? The algorithm uses the following strategy to answer this question:

1. For a given trishear model in the studied universe (gray dashed lines, Fig. 1), measure the difference between the observed (black ticks, Fig. 1) and the modeled (gray ticks, Fig. 1) beds at all data locations along the profile ($i=1,\ldots,n$). The algorithm uses two criteria to evaluate this difference: bedding dip (θ) and bedding location (x, y; Fig. 1).
2. Create a summary (overall) statistic that shows the total difference in bedding dip and location between the data observed and the predicted model. The algorithm uses a chi-square statistic (Press et al., 1986) to compute the total difference:

$$\chi^2 = \sum_i^n \frac{(x_{oi} - x_{mi})^2}{(x_{oi} + x_{mi})} + \sum_i^n \frac{(y_{oi} - y_{mi})^2}{(y_{oi} + y_{mi})} + \sum_i^n \frac{(\theta_{oi} - \theta_{mi})^2}{(\theta_{oi} + \theta_{mi})} \quad (1)$$

where the subscripts o and m stand for observed and modeled, respectively (Fig. 1).

3. Repeat steps 1 and 2 for all trishear models in the universe.
4. Choose the trishear model that minimizes the total difference in bedding dip and location, producing the lowest difference achievable by *any* trishear model in the universe. The algorithm chooses the model with the minimum chi-square value.

The algorithm requires the input of (Fig. 1): (i) the coordinates of the points used to digitize the profile, (ii) the location of bedding observations along the profile (x_{oi}, y_{oi}), (iii) bedding dips (θ_{oi}), (iv) the horizontal location at which the undeformed stratigraphy (the stratigraphy outside the fold) is defined (x_s), and (v) the vertical coordinate (y_{ui}) and regional dip (θ_{ui}) of the beds in the area outside the fold. The last three parameters define the undeformed layer template (the initial layer cake geometry). If x_s is in the footwall area, the undeformed layer template is the same for all tested trishear models. If x_s is in the hanging wall area, the coordinates of the layer template (x_{ui}, y_{ui}) are updated for each trishear model:

$$x_{ui(\text{updated})} = x_{ui(\text{input})} - s\cos(\alpha) \quad (2)$$

$$y_{ui(\text{updated})} = y_{ui(\text{input})} - s\sin(\alpha) \quad (3)$$

where s and α are the fault slip and ramp angle of the currently tested trishear model.

The user should also specify the extent of the universe by entering a grid search matrix consisting of the minimum value, the maximum value, and the step increment of: (i) horizontal coordinate of the fault tip (x_t), (ii) vertical coordinate of the fault tip (y_t), (iii) ramp angle, (iv) *P*/*S* ratio, (v) trishear angle, and (vi) fault slip. The algorithm then searches over the specified range of values for the trishear model that best fits the transect data. The statistics of the grid search and the best-fit model are delivered to a text file. Either homogenous or heterogeneous trishear (Zehnder and Allmendinger, 2000) can be implemented. For simplicity, only homogeneous trishear is considered in this paper.

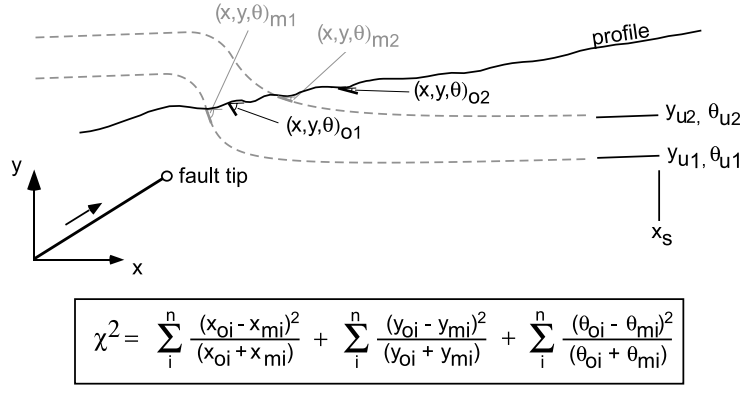

Fig. 1. Elements of the strategy used to fit trishear models to bedding data along a topographic profile. For a given trishear model in the studied universe (gray dashed lines), differences in bedding dip (θ) and bedding location (x, y) between the actual (black ticks) and the modeled (gray ticks) beds are computed using a chi-square statistic (enclosed equation). This procedure is repeated for all trishear models in the universe. The best trishear model is the one that minimizes chi-square.

3. Test of the algorithm

A simple trishear forward model was used to test the robustness of the algorithm along an arbitrary profile (Fig. 2). The first objective of this exercise is to see if the best-fit model parameters identified by the algorithm (i.e. grid search) are the same as the parameters input to the forward model. The second objective of this test is to see if the best-fit solution is unique, or if there are local minima in the grid search space that could be mistaken for the global minimum. Modeling a synthetic fold geometry generated with known parameters might seem circular, but in fact it is the only test for which one can evaluate with 100% confidence the success of the algorithm. Actual fold cases will always have errors (observations, measurements, interpretations, etc.), but synthetic folds do not.

The locations of input data are highlighted in gray in Fig. 2. Notice that the stratigraphy in this exercise is defined in the footwall area outside the fold. The ramp angle and the fault tip location are assumed to be known. Hence, the algorithm searches for the best-fit model over a reasonable range of *P*/*S* ratio, trishear angle, and fault slip. The table in Fig. 2 lists the grid search matrix; 35301 unique combinations were tested. This yields a three-dimensional (3-D) matrix of chi-square values, with dimensions of fault slip, trishear angle, and *P*/*S* ratio.

Two-dimensional slices through the 3-D matrix of chi-square values illustrate the effectiveness of the grid search (Fig. 3). The best-fit parameters are exactly those used in the forward model, and there are no local minima in the grid search space. Fig. 3a shows that *P*/*S* ratio and trishear angle are inversely correlated (as also noted in Allmendinger et al., 2004). At the best slip value, the bedding data can be fit with a low *P*/*S* ratio and high trishear angle or vice versa. This correlation is characteristic of the grid search (grid searches along flat, left sloping, right sloping, concave downward, and concave upward profiles all display the same statistical trend). Fig. 3b and c shows that the solution for the best slip is not very well constrained. At the correct values of *P*/*S* ratio and trishear angle, the transect data can be fit by a range of slip values ± 20 units of the correct slip. This results because all the bedding intersections in this example lie inside the fold (Fig. 2). In contrast, grid searches along profiles that cross beds in the hanging wall and/or footwall areas outside the fold have robust solutions for slip. In these cases, finding the best-fit slip requires nothing more than determining the correct throw (Allmendinger et al., 2004). In general, the success of the search relies on the completeness of coverage of the structure along the transect, the number of bedding observations, and the step size of the parameters included in the search. More demanding searches were also conducted for unknown ramp angle and fault tip location. In these cases, the best fit parameters were exactly or close to those used in the forward model, depending on the step increments in ramp angle and *x* and *y* fault tip locations.

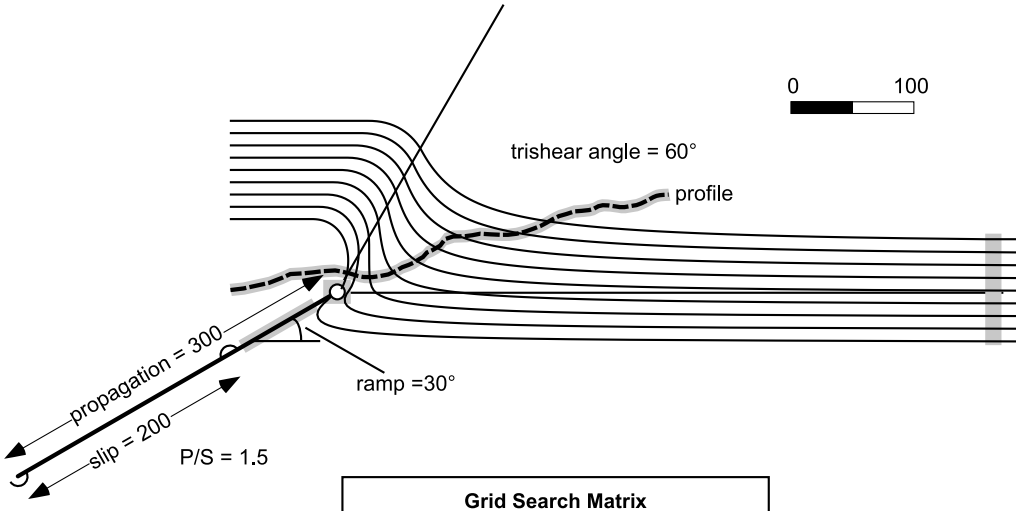

Grid Search Matrix

Parameter	Minimum	Maximum	Step
Slip	100	300	5
Trishear angle	20	100	2
P/S	0.5	2.5	0.1

35301 combinations tested

Fig. 2. Forward trishear model used to test the algorithm. The areas of input data are highlighted in gray. The table below shows the range of values used in the grid search. The parameters included in the search are: (i) *P*/*S* ratio, (ii) trishear angle, and (iii) fault slip. The success of the grid search is indicated by how close the computed best-fit parameters are to those input to the forward model.

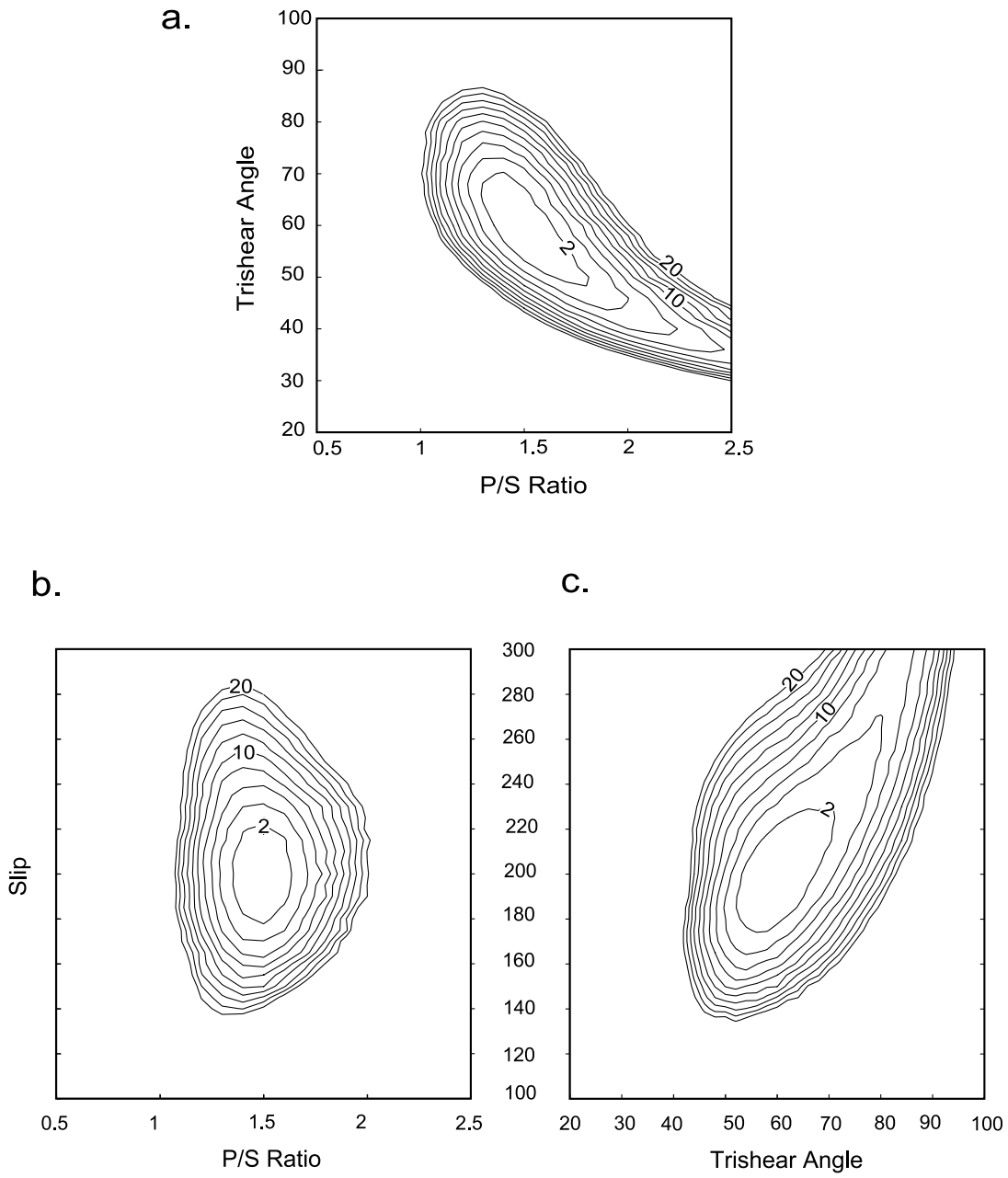

Fig. 3. Two-dimensional slices through the 3-D matrix of chi-square values produced by grid searching over the range of values shown in Fig. 2. Slices are constructed at (a) best displacement (200 units), (b) best trishear angle (60°), and (c) best *P*/*S* ratio (1.5). In each diagram, contours are in intervals of two chi-square values.

4. Application

The application of the algorithm is shown by modeling a previously published transect of the Waterpocket monocline in southern Utah (Bump, 2003; Fig. 4a and b). The Waterpocket monocline forms the eastern limb of the Circle Cliffs uplift. The fold extends along strike for more than 50 km. Across strike, the wavelength of the fold (the horizontal distance between the flat lying hanging wall and the flat lying footwall) is about 8 km (Davis, 1999; Fig. 4a and b). The surface exposure of the monocline is excellent, and therefore its surface geometry is very well constrained (Fig. 4b). The subsurface structure and the geometry of the underlying fault, however, are unknown. The monocline is an ideal case for applying the algorithm.

The footwall area outside the fold is used to define the 'undeformed' stratigraphy (Fig. 4b). Fig. 4c shows the parameter ranges used in the grid search. All six parameters, fault tip location, ramp angle, *P*/*S* ratio, trishear angle, and slip, were searched (the dashed rectangle in Fig. 4b indicates the area where the location of the fault tip was searched). 96525 unique combinations were tested.

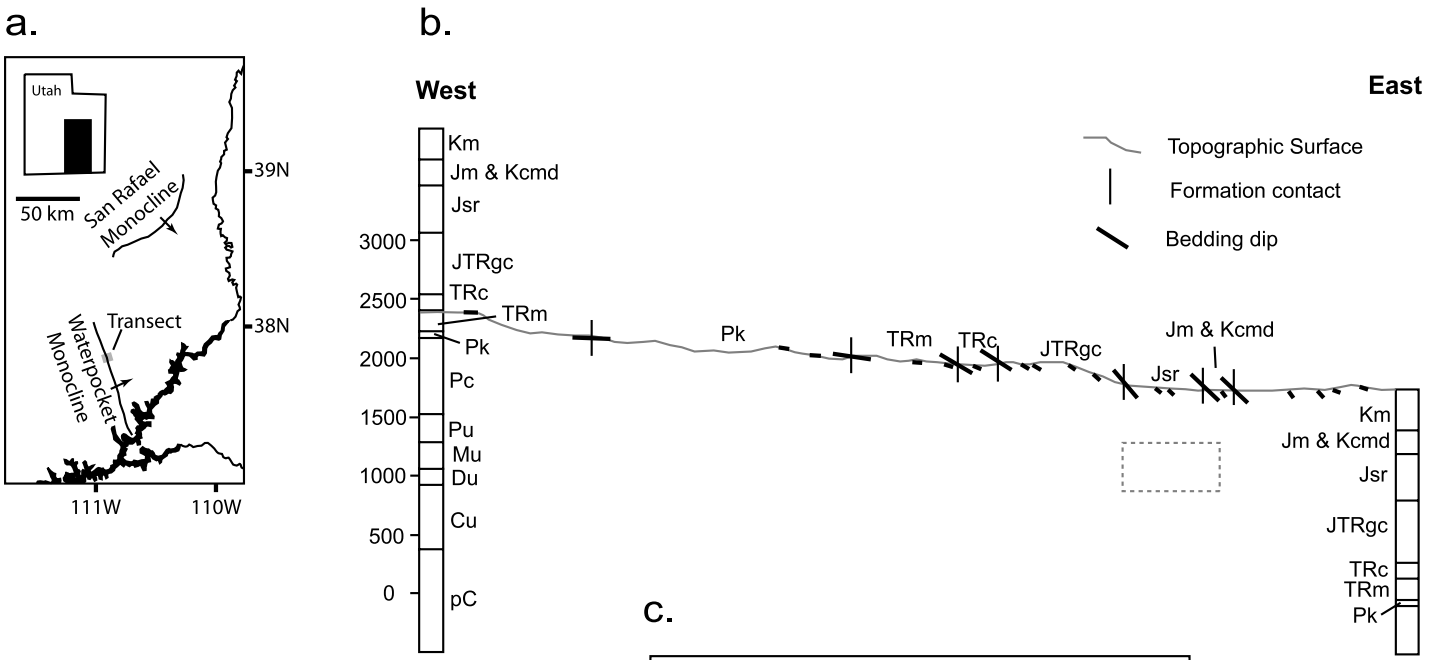

Grid Search Matrix

Parameter	Minimum	Maximum	Step
Slip (m)	3000	5000	200
Trishear angle	60	120	5
P/S	1.0	3.0	0.25
Ramp angle	20	40	5
Tipline Y (m)	870	1270	200
Tipline X (m)	5800	6600	200

96525 combinations tested

Fig. 4. (a) Location of the Waterpocket and San Rafael monoclines, simplified from Davis (1999). Lines with arrows show the upper hinge of the monoclines. Arrows show the vergence of the monoclines. Gray area indicates the location of the transect. (b) Transect data of the Waterpocket monocline from Bump (2003). Elevations are in meters above sea level and the transect is drawn without vertical exaggeration. The stratigraphy on each side of the transect is based on well logs and projection from the surface. The dashed rectangle in the cross-section shows the area where the location of the fault tip was searched. (c) Grid search matrix used to find the trishear model that best fits the transect data of the Waterpocket monocline.

The best model fits very well the transect data, and reasonably well the stratigraphy in the hanging wall and footwall areas outside the fold (Fig. 5a). The best model has a ramp angle of 35°, a *P*/*S* of 2.25, a trishear angle of 105°, and fault slip of 3.8 km (Fig. 5a and b). Two-dimensional slices at the best fault tip location and ramp angle show that the solution is better constrained in *P*/*S* ratio than in trishear angle (Fig. 5b, left), and that the solution for the best slip is very robust (Fig. 5b, center and right). This is because the Kaibab limestone (Pk)–Moenkopi Formation (TRm) contact outcrops both in the forelimb and in the hanging wall area outside the fold (Fig. 4b). Only in models with slip values between 3.6 and 3.8 km is this contact intersected twice by the profile (Fig. 5a and b).

Refined searches for ramp angle (holding constant the fault tip location), or *P*/*S* ratio and trishear angle (holding constant the fault tip location and the ramp angle) lead to minor variations in parameter values. A trishear model that fits the Waterpocket monocline must have a ramp angle of about 35°, a *P*/*S* ratio between 2.2 and 2.3, a high trishear angle (between 100° and 110°), and fault slip of about 3.8 km. Trishear modeling of the Waterpocket monocline transect data therefore suggests that the fault started to propagate well below the basement-cover contact (the initial

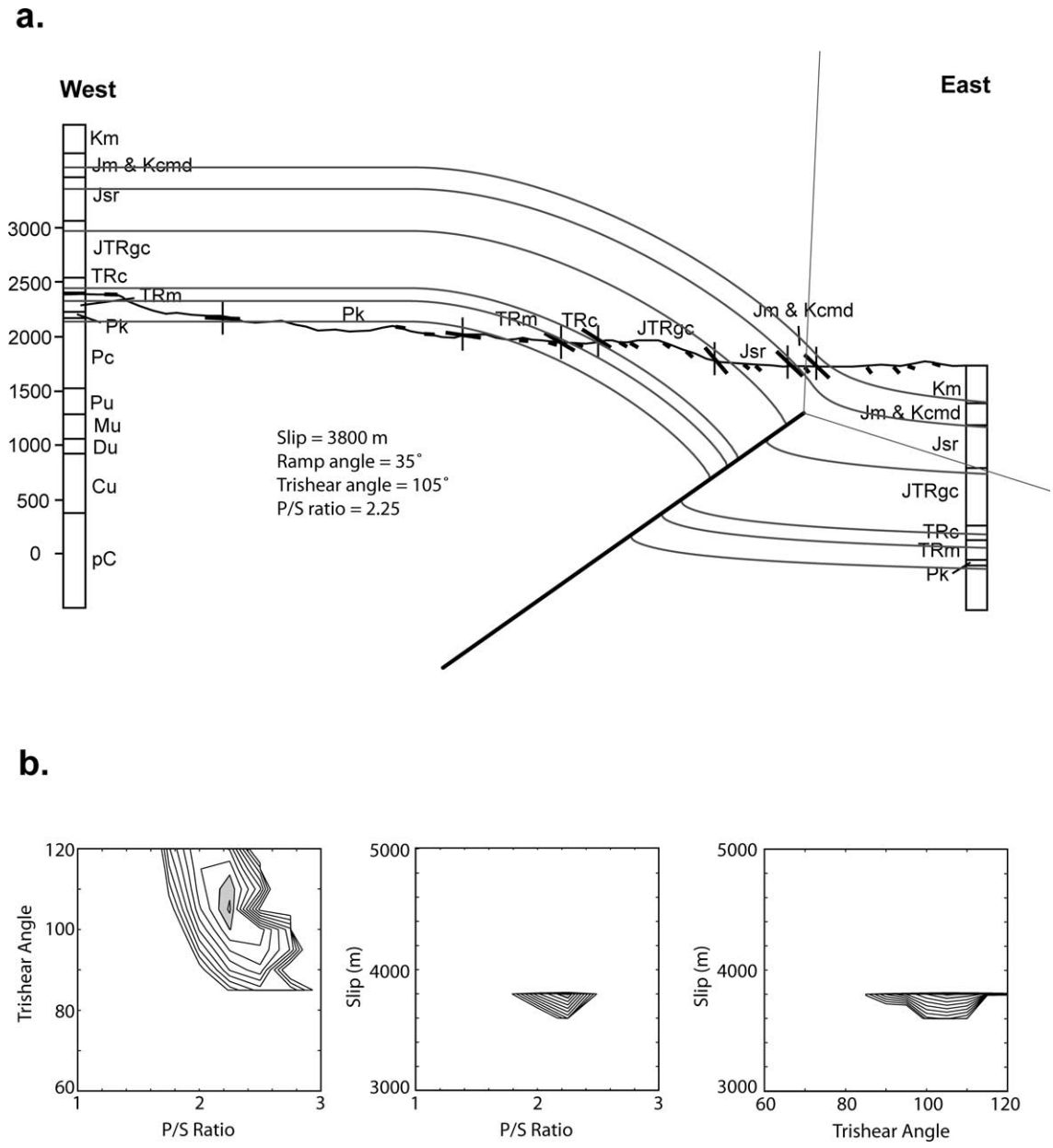

Fig. 5. (a) Best fit trishear model of the Waterpocket monocline. (b) Summary of the statistics of the grid search. Two-dimensional slices are constructed at the best location of the fault tip and best ramp angle (35°). The left slice is drawn at the best displacement (3800 m), the center slice is drawn at the best trishear angle (105°), and the right slice is drawn at the best *P*/*S* ratio (2.25). In each plot, contours are in intervals of five chi-square values. Gray areas indicate the models with chi-square values less than 10.

location of the fault tip must be at least 3.5 km below the basement-cover contact in the hanging wall). Bump (2003) arrived at a similar conclusion (for the Waterpocket and San Rafael monoclines; Fig. 4a) using a preliminary (and more restricted) version of my unpublished algorithm. Based on this conclusion, he postulated that some of the faults that underlie the Laramide uplifts originated as footwall shortcuts of reactivated listric normal faults (Bump, 2003).

The best fit model (Fig. 5) matches fairly well the observable features of the Waterpocket monocline. There is little change in layer thickness from the upper backlimb (borehole data), through the middle limb (exposed section), into the flat lying lower limb (borehole data; Bump, 2001). Most of the thickness changes occur in the immediate footwall of the fault. A plausible, yet untested alternative interpretation of the Waterpocket monocline is that it is a parallel fold. The purpose of this exercise, however, is not to discuss the ultimate origin of the Waterpocket monocline, but rather to illustrate the application of the algorithm to a real structure.

5. Conclusions

In this note, a simple yet powerful algorithm has been presented to fit trishear models to bedding data along a topographic profile. The application of the algorithm to both synthetic and actual transect data shows that the algorithm is robust and reliable. The algorithm significantly extends the applicability of the trishear model. The subsurface geometry of the fold and its accompanying fault, the amount of fault slip and fault propagation, and the position of fault

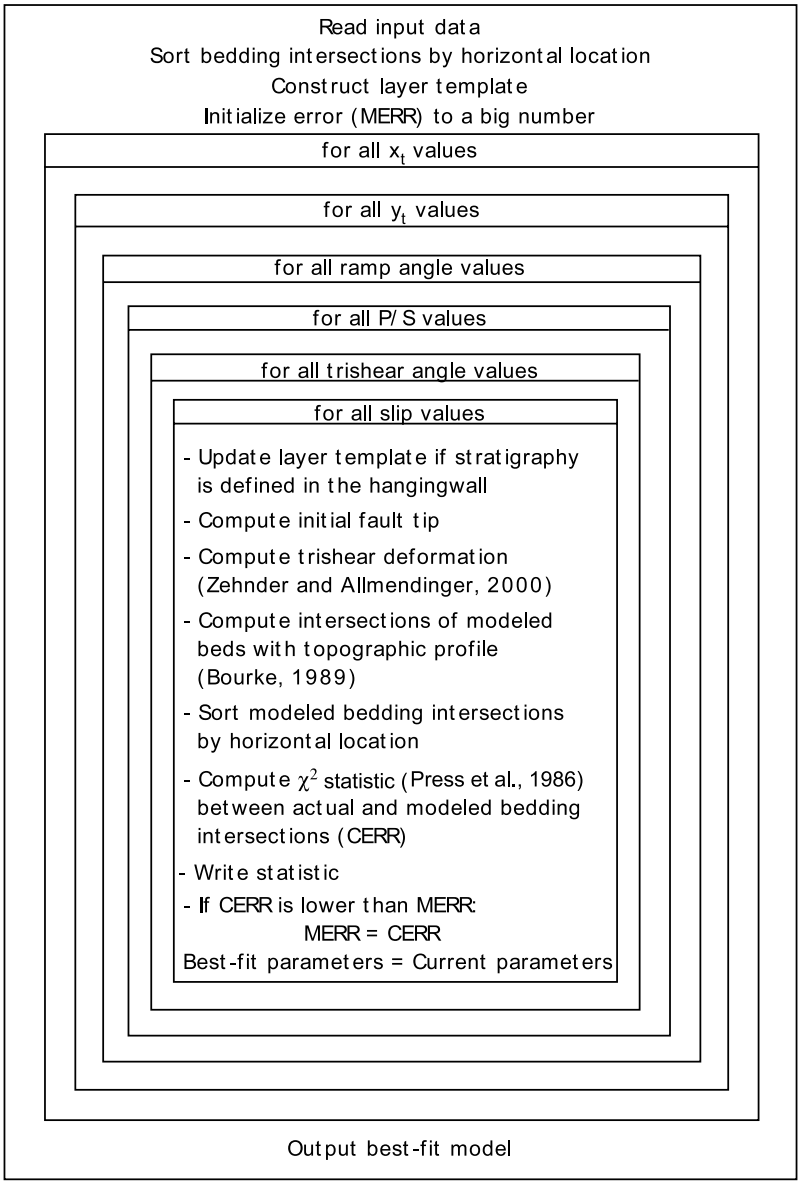

Fig. A1. Graphical representation of the algorithm.

nucleation; can all now be extracted from a set of scattered observations along a very restricted window in the structure. This type of information is critical in the evaluation of the seismic hazard posed by buried, active faults (Keller and Pinter, 2002), and in the assessment of the geometry and internal structure of petroleum reservoirs (Erslev and Mayborn, 1997).

Acknowledgements

This paper benefited from numerous constructive discussions with Richard Allmendinger and Jack Loveless. I thank Alex Bump for generously providing his data of the Waterpocket monocline, and Eric Erslev for carefully reviewing the manuscript. This work was supported by National Science Foundation grants EAR-9814348 to Richard Allmendinger, and EAR-0125557 to Richard Allmendinger and Alan Zehnder. Final modifications to the manuscript were made while holding a fellowship at the Norwegian Geotechnical Institute. Richard Allmendinger has implemented the algorithm in his program FaultFold 5.0© (Mac OS X platform). Through an elegant interface the user can interactively input the data, set the grid search matrix, and visualize the fitness of the best model.

Appendix A

Fig. A1 describes the implementation of the algorithm. The algorithm consists of six nested loops (each one corresponding to a grid search parameter). The main calculations are inside the loop for slip values. The calculation of trishear deformation is based on the homogeneous trishear velocity field of Zehnder and Allmendinger (2000, their equation 6). The strategy to determine the intersections of the modeled beds with the topographic profile is based on the Bourke (1989) algorithm. A straight insertion algorithm (Press et al., 1986) was used to sort the actual and modeled bedding intersections for comparison. The statistic that summarizes the differences between the actual and modeled beds (Eq. (1)) is based on Press et al. (1986).

References

Allmendinger, R.W., 1998. Inverse and forward numerical modeling of trishear fault-propagation folds. Tectonics 17 (4), 640–656.

Allmendinger, R.W., Zapata, T.R., Manceda, R., Dzelalija, F., 2004. Trishear kinematic modeling of structures with examples from the Neuquén basin, Argentina. In: McClay, K.R. (Ed.), Thrust Tectonics and Hydrocarbon Systems: AAPG Memoir. American Association of Petroleum Geologists, Tulsa, 82, pp 356–371.

Bourke, P., 1989. Intersection point of two lines. http://astronomy.swin.edu.au/~pbourke/geometry/lineline2d/.

Bump, A.P., 2001. Kinematics, dynamics, and mechanics of Laramide Deformation, Colorado Plateau, Utah and Colorado. Ph.D. thesis, University of Arizona.

Bump, A.P., 2003. Reactivation, trishear modeling, and folded basement in Laramide uplifts: Implications for the origins of intra-continental faults. GSA Today 13 (3), 4–10.

Davis, G.H., 1999. Structural geology of the Colorado Plateau region of Southern Utah with special emphasis on deformation bands. Geological Society of America, Special Paper 342.

Erslev, E.A., 1991. Trishear fault-propagation folding. Geology 19, 617–620.

Erslev, E.A., Mayborn, K.R., 1997. Multiple geometries and modes of fault propagation folding in the Canadian thrust belt. Journal of Structural Geology 19, 321–335.

Keller, E.A., Pinter, N., 2002. Active Tectonics, Earthquakes, Uplift, and Landscape, 2nd ed Prentice Hall, New Jersey.

Press, W.H., Flannery, B.P., Teukolsky, S.A., Vetterling, W.T., 1986. Numerical Recipes: The Art of Scientific Computing. Cambridge University Press, New York.

Suppe, J., Medwedeff, D.A., 1990. Geometry and kinematics of fault propagation folding. Eclogae Geologicae Helvetiae 83, 409–454.

Zehnder, A.T., Allmendinger, R.W., 2000. Velocity field for the trishear model. Journal of Structural Geology 22, 1009–1014.